

Vibration Step Test for Performance Analysis of Inertial Measurement Unit

Domenico Capriglione¹, Marco Carratù², Marcantonio Catelani³, Lorenzo Ciani³, Gabriele Patrizi³, Antonio Pietrosanto², Paolo Sommella²

¹ *Department of Information and Electrical Engineering "Maurizio Scarano", University of Cassino and Southern Lazio, Via G. Di Biasio, 43, Cassino (FR), Italy, capriglione@unicas.it*

² *Department of Industrial Engineering, University of Salerno, Via Giovanni Paolo II, 132, Fisciano (SA), Italy, {mcarratu, apietrosanto, psommella}@unisa.it*

³ *Department of Information Engineering, University of Florence, Via di S. Marta, 3, 50139, Florence, Italy, {marcantonio.catelani, lorenzo.ciani, gabriele.patrizi}@unifi.it*

Abstract – Nowadays Inertial Measurement Units are largely implemented in several applications, such as automotive and self-driving vehicles, Unmanned Aerial Vehicles, cellular phones, robotics, artificial intelligence and many others. Despite this, recent literature doesn't cover properly both the characterization of the dynamical metrological performances and the reliability analysis when microelectronic devices operate under real environmental conditions. Trying to fill this gap, the characterization of an Inertial Measurement Unit under vibration condition is proposed in this work by means of a step-test vibration profile to test the behavior of an inertial platform subjected to a sinusoidal vibration at different frequencies. Starting from the widely known sine sweep vibration profile, a customized test plan has been developed basing on a frequency step up of a sinusoidal stimulus over time to investigate the frequency response of the inertial platforms. The application to a set of real devices has confirmed that the proposed test allows identifying the effects of mechanical stress on the metrological performances of microelectromechanical sensors over a frequency domain. The developed test plan could also be used to investigate whether or not sinusoidal vibrations at certain frequencies trigger some failure mechanisms that are normally quiescent.

Keywords – *Diagnostic; Inertial Measurement Unit; MEMS; Testing; Vibration.*

I. INTRODUCTION

In the last few years diagnostic and fault diagnosis have become a crucial requirement in many industrial fields because they allow to increase both reliability and availability of a complex system [1], [2]. Moreover, the

need for corrective maintenance is minimized when a proper condition monitoring tool and an effective diagnostic system are designed, as well as the overall management costs [3]–[5]. In many practical situations, Inertial Measurement Units (IMUs) represents an optimal trade-off to achieve the design requirements and implement effective and efficient diagnostic [6], [7].

IMUs are largely employed in many practical applications, such as cellular phones, automotive industry, human motion, robotics, transportation vehicles, military equipment and Unmanned Aerial Vehicles [8]–[10].

Consequently, the accuracy and reliability of such systems become a fundamental topic for assuring the expected behaviour and the correct operating of all those systems based on IMUs.

The commercial IMUs usually integrate the following sensors:

- A triaxial accelerometer used to measure the linear acceleration toward the three axes;
- A triaxial gyroscope to acquire information on the angular rate of the system toward the three axes;
- A triaxial magnetometer in order to measure the static magnetic field.

MEMS (Micro-Electro-Mechanical-Systems) technology leads the market of inertial measurement platform due to the small dimension, ease integration, low power dissipation, low-cost, high accuracy and high stability [11], [12].

The effects of the operating conditions on the dynamic metrological performances and on the reliability parameters is a fundamental topic that recent MEMS-based IMUs literature barely considers. The real scenario in which the IMU is operating is a key element during the system design that must be taken into account. Relevant temperature variation, high humidity level, significant vibrations, mechanical shocks are only a few list of

environmental factor that deeply affect the performances of microelectronic devices [13]–[15].

This work presents a new vibration test-plan and a measurement setup in order to test the frequency response of a widely-used MEMS-based IMU in case of vibration stress at different frequencies. Currently, no international standards regarding specifically the test of IMUs or MEMS devices are available. Consequently, starting from preliminary experimental results shown in [16], [17], in this paper a new test procedure under vibration stress is proposed merging the information included in several generic standards. The aim of the test is the characterization of the IMU frequency response using the so-called step test.

A set of inertial measurement platforms each one involving three triaxial microelectromechanical sensors (i.e. one accelerometer, one gyroscope and one magnetometer) were designed and tested by means of a vibration shaker to simulate vibrations stimuli that are quite common during transportation and shipment of such devices. The vibration profile was also designed to be well representative of the real vibration conditions during the normal operations of complex systems in different applications.

The final part of the paper illustrates some measurement results of the tests carried out at the Analytical CETACE test laboratory located in Scandicci, Florence (Italy).

II. VIBRATION STEP TEST

The objective of this work was to test the frequency behavior of an inertial platform subjected to a sinusoidal vibration at different frequencies, maintaining a constant peak acceleration.

Starting from the widely known sine sweep vibration profile, a customized test plan was developed in this work basing on a frequency step-up of a sinusoidal stimulus over time to carefully investigate the frequency response of the inertial platforms. The developed test plan is a sort of vibration step-test, where the physical quantity that step up is not the peak acceleration but is the frequency of the stimulus.

Using this test profile, it is possible to achieve information about the frequency response of the IMU under test and, at the same time, it is possible to investigate its to withstand a constant vibration stimulus over a large frequency span. The latter could also provide significant information on the reliability performances of the IMUs, which represents a critical requirement in many application fields.

The classical sinusoidal sweep vibration test is defined and illustrated in many international standards, such as the European standard IEC 60068-2-6 (2009) [18], the global standard for the microelectronics industry JESD22-B103B.01 (2016) [19] and the military standard MIL-

STD-810G (2008) [20] regarding the environmental engineering considerations and laboratory tests of electronic equipment. Based on the previous standards, the vibration step test adopted in this work consists of a single sweep from 40 Hz to 2000 Hz analyzing a single frequency for a fixed period of holding time. After such a period of time, the frequency will be increase of a fixed frequency step. The severity of the test is the following

- Minimum frequency: 40 Hz
- Maximum frequency: 2000 Hz
- Frequency step: 20 Hz
- Vibration peak: 2 g
- Type of vibration stimuli: Sinusoidal
- Holding time at each step: 25 s
- Number of cycles: 1
- Number of axes: 3

An extract of the vibration profile proposed in this work is illustrated in figure 1, considering only the subrange 40 – 200 Hz.

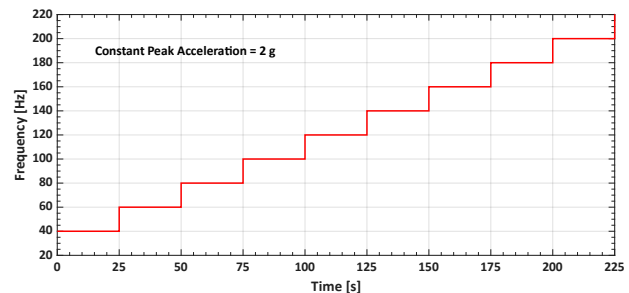


Fig. 1. Extract of the vibration step-test profile in the frequency range 40-200 Hz.

III. EQUIPMENT UNDER TEST

In order to improve the reliability of the measurement setup, the experimental setup is composed of the following components:

- Three MEMS Inertial Measurement Units which are the Devices Under Test (DUTs). Each DUT integrates three MEMS sensors. The integrated triaxial accelerometer is characterized by a linear acceleration full scale of $\pm 2g/\pm 4g/\pm 8/\pm 16$ g, and it can achieve a sensitivity of 0.732 mg/LSB in case the highest full scale is selected. The integrated triaxial gyroscope is characterized by an angular rate full scale of $\pm 245/\pm 500/\pm 2000$ dps reaching a sensitivity of 70 mdps/LSB when it operates at ± 2000 dps full scale. Each IMU also integrates a triaxial magnetometer characterized by a magnetic field full scale of $\pm 4/\pm 8/\pm 12/\pm 16$ gauss and a sensitivity of 0.58 mgauss/LSB if the highest full scale is selected.
- Three Nucleo-64 developing boards by

“STMicroelectronics” based on a STM32F401RE microcontroller [21]. Each DUT is connected to one Nucleo-64 board to ensure the highest performances. The primary purposes of the controller are the following:

- To initialize and set all the DUT functionalities.
- To acquire data coming from the MEMS sensors. The communication between the DUT and the microcontroller is based on the I2C communication bus, which operates at 400 kHz.
- To transfer the acquired data to a PC through the USB communication interface, which implements a virtual COM port service operating at 115200 bps. The output data rate (ODR) selected for this application is 100 Hz since it is a classical choice for many positioning algorithms [22]. In this case, an analog antialiasing filter of 50 Hz is automatically introduced on each axis and on each sensor.
- A computer equipped with suitable software responsible for collecting and storing the data measured by the DUTs.

Moreover, to implement the vibration profile described in the previous section, the test setup requires other equipment. In particular, a vibration shaker with the frequency range and acceleration peak suitable to fulfill the proposed test has been used. The shaker must be connected to a digital controller that continuously monitors the acceleration provided by the shaker by means of at least two piezoelectric accelerometers. Moreover, the controller regulates the work of the shaker using a feedback channel in order to ensure that the vibration stimuli are constantly in compliance with the proposed test plan. The complete test setup is illustrated in figure 2.

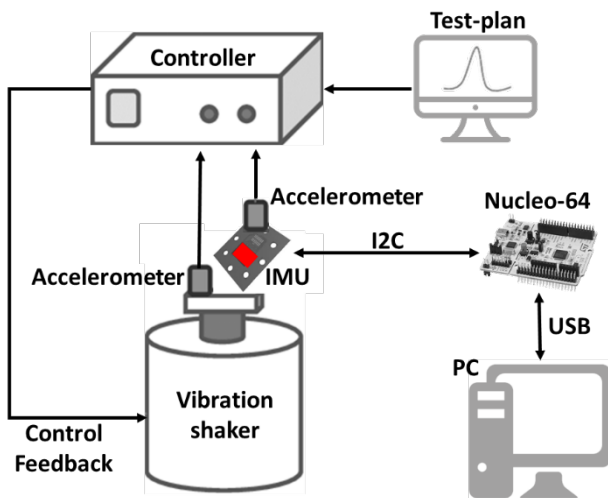


Fig. 2. Schematic representation of the implemented experimental setup composed by a vibration shaker, a controller, two accelerometers, IMU, Nucleo64, and a PC.

For the sake of simplicity, only one pair of IMU-Nucleo64 is illustrated in the figure, while the real setup included three pairs of IMU-Nucleo64, each one connected to the computer for data acquisition and storage.

IV. RESULTS AND DISCUSSIONS

The experiment went toward two different kinds of tests, reporting the first results regarding the behavior of the three identical IMUs under the step sine test described in section III.

More in detail, considering Fig. 3, where the accelerometer’s output of the DUT #1 during the entire test is showed, three different operation zones can be defined:

- The Before Test (BT) zone, representing the instants before the application of the step sine test.
- The After Test (AT) zone, representing the instants after the application of the step sine test
- The Test Zone, where the step sine test is applied.

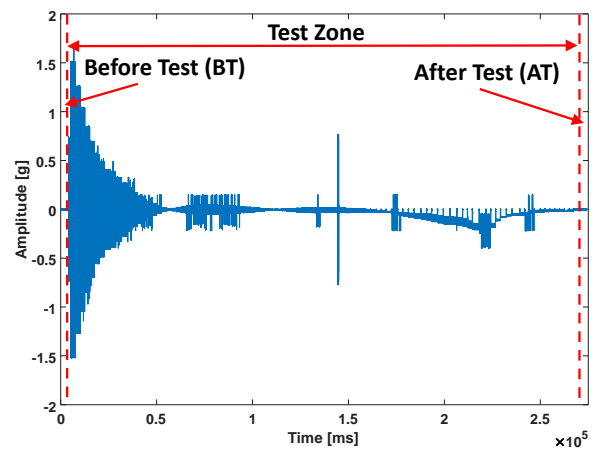


Fig. 3. Scheme of the zones for the experimental tests considering, for example, the accelerometer’s output of DUT #1.

The first part of the experimental test aims to evaluate the destructive or the miss calibration effect of the test on the devices under investigation, the reason why it considers only analyses of the BT and AT zones for each sensor of every IMUs (i.e. accelerometer and gyroscope).

In Tables I-III have reported the average values, and the standard deviations for each zone previously defined. As can be seen from the Tables I-III, the measured value show for each sensor axis of both the accelerometer and gyroscope, full compatibility of the results achieved in the zones AT with BT for every step sine excitation applied on all the axes (respectively, excitation on X-axis, Table I, excitation on Y-axis, Table II, and excitation on Z-axis, Table III). This fact represents two fundamental results: i)

Table I. Mean and standard deviation of X- axis sensors outputs for the analyses "Before-After".

Excitation on axis	DUT	Accelerometer [g]				Gyroscope [°/s]			
		Before Test		After Test		Before Test		After Test	
		μ	σ	μ	σ	μ	σ	μ	σ
X	#1	0.000	0.000	0.000	0.001	-0.014	0.133	0.032	0.129
	#2	0.000	0.002	0.000	0.002	0.013	0.108	-0.153	0.126
	#3	-0.001	0.002	0.000	0.002	0.018	0.105	0.023	0.112
Y	#1	0.000	0.001	0.000	0.001	-0.032	0.105	-0.089	0.092
	#2	0.000	0.002	0.000	0.002	0.009	0.113	-0.154	0.107
	#3	0.000	0.001	0.000	0.001	0.003	0.074	0.060	0.094
Z	#1	0.000	0.002	-0.001	0.002	0.000	0.127	-0.023	0.099
	#2	0.000	0.002	-0.001	0.002	0.001	0.117	-0.026	0.110
	#3	0.000	0.001	0.000	0.002	-0.015	0.094	-0.005	0.089

Table II. Mean and standard deviation of Y- axis sensors outputs for the analyses "Before-After".

Excitation on axis	DUT	Accelerometer [g]				Gyroscope [°/s]			
		Before Test		After Test		Before Test		After Test	
		μ	σ	μ	σ	μ	σ	μ	σ
X	#1	0.000	0.000	0.000	0.001	-0.014	0.133	0.032	0.129
	#2	0.000	0.002	0.000	0.002	0.013	0.108	-0.153	0.126
	#3	-0.001	0.002	0.000	0.002	0.018	0.105	0.023	0.112
Y	#1	0.000	0.001	0.000	0.001	-0.032	0.105	-0.089	0.092
	#2	0.000	0.002	0.000	0.002	0.009	0.113	-0.154	0.107
	#3	0.000	0.001	0.000	0.001	0.003	0.074	0.060	0.094
Z	#1	0.000	0.002	-0.001	0.002	0.000	0.127	-0.023	0.099
	#2	0.000	0.002	-0.001	0.002	0.001	0.117	-0.026	0.110
	#3	0.000	0.001	0.000	0.002	-0.015	0.094	-0.005	0.089

Table III. Mean and standard deviation of Z- axis sensors outputs for the analyses "Before-After".

Excitation on axis	DUT	Accelerometer [g]				Gyroscope [°/s]			
		Before Test		After Test		Before Test		After Test	
		μ	σ	μ	σ	μ	σ	μ	σ
X	#1	0.000	0.000	0.000	0.001	-0.014	0.133	0.032	0.129
	#2	0.000	0.002	0.000	0.002	0.013	0.108	-0.153	0.126
	#3	-0.001	0.002	0.000	0.002	0.018	0.105	0.023	0.112
Y	#1	0.000	0.001	0.000	0.001	-0.032	0.105	-0.089	0.092
	#2	0.000	0.002	0.000	0.002	0.009	0.113	-0.154	0.107
	#3	0.000	0.001	0.000	0.001	0.003	0.074	0.060	0.094
Z	#1	0.000	0.002	-0.001	0.002	0.000	0.127	-0.023	0.099
	#2	0.000	0.002	-0.001	0.002	0.001	0.117	-0.026	0.110
	#3	0.000	0.001	0.000	0.002	-0.015	0.094	-0.005	0.089

the step sine test applied has not damaged both the accelerometers and the gyroscopes, ii) also in terms of sensor calibration (see the average values), the tests seem not to affect both of them.

The second part of the experimental test has the aim of investigating the operation of the IMU with the application

of frequency increasing sine step test.

For this reason, in those experiments, the region considered in Fig.3 is the one represented in the middle, labeled Test Zone. For the sake of brevity, the analysis will regard only the accelerometer's outputs for the three identical DUTs.

The experimental results are reported in Figs 4-6, where the RMS values, over each single step sine length window, are shown. First of all, looking at the figures previously mentioned, it can be seen that independently from the axis on which the stimulus is applied, all the accelerometer's axes, not interested directly by the excitation (for example in Fig. 4 where the stimulus is applied on the X-axis, consider the Y and Z axes), show an unexpected behavior: their outputs are significantly different from zero, a fact that means the presence of an undesired cross-axis sensitivity. The second significant result is retrieved, analyzing all the axes outputs: also if an output data rate has been set to 100Hz, which automatically introduce a low-pass filter on the outgoing data at ODR/2 (50 Hz), the outputs measured by the sensors follow the expectation up to 400 Hz stimulus; after that, the outputs of all the axis start present suddenly gains and not linear behaviors.

Furthermore, it is important to highlight the operation of all the axes with high frequencies stimulus: all the sensors axes measure high acceleration levels, which are not expected. While the worst behavior seems to be exhibited by the application of stimulus on the z-axes, the same results, previously mentioned, have been obtained for all the DUTs under test, confirming the presence of an important deviation of the operation from the expected one. Also, for the gyroscopes, similar considerations can be drawn from the analysis of RMS values achieved over the step sine tests.

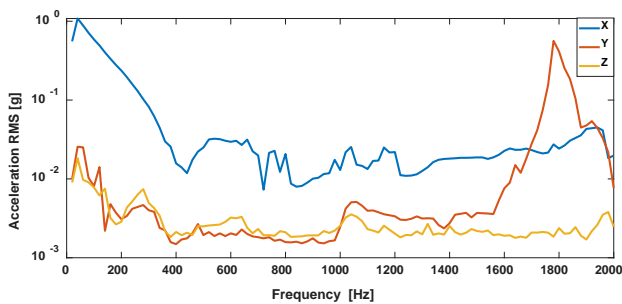


Fig. 4. RMS accelerometer's output with stimulus applied to the x-axis.

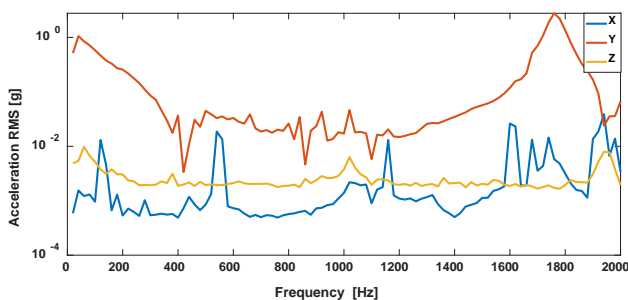


Fig. 5. RMS accelerometer's output with stimulus applied to the y-axis.

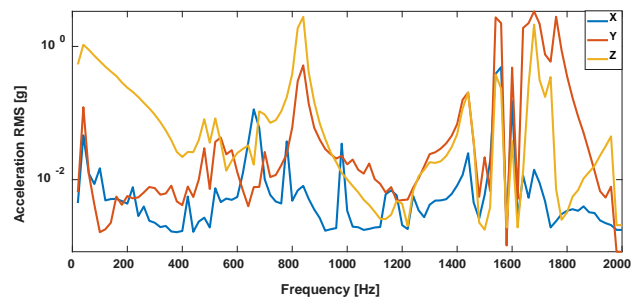


Fig. 6. RMS accelerometer's output with stimulus applied to the z-axis.

V. CONCLUSIONS

The paper has shown the application of a novel vibration sine step test on a popular and commercial IMU. Besides a classical testing approach aimed at verifying the eventuality of device damaging and missing of calibration, the proposed tests have allowed analyzing the operation of accelerometers and gyroscopes during the application of the vibration stimulus, thus highlighting unexpected comportment as cross axes sensitivity and incorrect operations under the high-frequencies stimulus. These results should lead to the design of new kinds of tests for those particular devices with the aim of analyzing their proper working under operating conditions experienceable in practice.

REFERENCES

- [1] D. Capriglione, M. Carratu, A. Pietrosanto, and P. Sommella, "Online Fault Detection of Rear Stroke Suspension Sensor in Motorcycle," *IEEE Trans. Instrum. Meas.*, vol. 68, no. 5, pp. 1362–1372, May 2019, DOI: 10.1109/TIM.2019.2905945
- [2] D. Capriglione, M. Carratu, A. Pietrosanto, and P. Sommella, "Real-time implementation of an IFD scheme for motorcycle sensors," *2018 IEEE International Instrumentation and Measurement Technology Conference (I2MTC)*, 14-17 May 2018, DOI: 10.1109/I2MTC.2018.8409833
- [2] M. Blanke, M. Kinnaert, J. Lunze, and M. Staroswiecki, *Diagnosis and Fault-Tolerant Control*. Berlin, Heidelberg: Springer Berlin Heidelberg, 2016.
- [3] L. Ciani, A. Bartolini, G. Guidi, and G. Patrizi, "Condition Monitoring of Wind Farm based on Wireless Mesh Network," in *16th IMEKO TC10 Conference 2019 - Testing, Diagnostics and Inspection as a Comprehensive Value Chain for Quality and Safety*, 2019, pp. 39–44.
- [4] A. Jablonski, Z. Dworakowski, K. Dziedzic, and F. Chaari, "Vibration-based diagnostics of epicyclic

- gearboxes – From classical to soft-computing methods,” *Measurement*, vol. 147, p. 106811, Dec. 2019.
- [5] P. Qian, X. Ma, D. Zhang, and J. Wang, “Data-driven condition monitoring approaches to improving power output of wind turbines,” *IEEE Trans. Ind. Electron.*, vol. 66, no. 8, pp. 1–1, 2018.
- [6] D. Capriglione *et al.*, “Experimental analysis of IMU under vibration,” in *16th IMEKO TC10 Conference 2019 - Testing, Diagnostics and Inspection as a Comprehensive Value Chain for Quality and Safety*, 2019.
- [7] J. Botero-Valencia, D. Marquez-Viloria, L. Castano-Londono, and L. Morantes-Guzmán, “A low-cost platform based on a robotic arm for parameters estimation of Inertial Measurement Units,” *Measurement*, vol. 110, pp. 257–262, Nov. 2017.
- [8] G. Dissanayake, S. Sukkarieh, E. Nebot, and H. Durrant-Whyte, “The aiding of a low-cost strapdown inertial measurement unit using vehicle model constraints for land vehicle applications,” *IEEE Trans. Robot. Autom.*, vol. 17, no. 5, pp. 731–747, 2001.
- [9] Q. He, C. Zeng, X. He, X. Xu, and Z. Lin, “Calibrating accelerometers for space-stable inertial navigation systems at system level,” *Measurement*, vol. 127, pp. 472–480, Oct. 2018.
- [10] G. E. Kang and M. M. Gross, “Concurrent validation of magnetic and inertial measurement units in estimating upper body posture during gait,” *Measurement*, vol. 82, pp. 240–245, Mar. 2016.
- [11] G. A. Aydemir and A. Saranlı, “Characterization and calibration of MEMS inertial sensors for state and parameter estimation applications,” *Measurement*, vol. 45, no. 5, pp. 1210–1225, Jun. 2012.
- [12] B. Alandry, L. Latorre, F. Mailly, and P. Nouet, “A CMOS-MEMS Inertial Measurement Unit,” in *2010 IEEE Sensors*, 2010, pp. 1033–1036.
- [13] L. Ciani, D. Galar, and G. Patrizi, “Improving context awareness reliability estimation for a wind turbine using an RBD model,” in *2019 IEEE International Instrumentation and Measurement Technology Conference (I2MTC)*, 2019, pp. 1–6.
- [14] L. Ciani and G. Guidi, “Application and analysis of methods for the evaluation of failure rate distribution parameters for avionics components,” *Measurement*, vol. 139, pp. 258–269, Jun. 2019.
- [15] D. Galar, “Context driven maintenance: an eMaintenance approach,” *Manag. Syst. Prod. Eng.*, vol. 3, no. 15, pp. 112–120, 2014.
- [16] D. Capriglione *et al.*, “Characterization of Inertial Measurement Units under Environmental Stress Screening,” in *2020 IEEE International Instrumentation and Measurement Technology Conference (I2MTC)*, 2020, DOI: 10.1109/I2MTC43012.2020.9129263
- [17] D. Capriglione *et al.*, “Development of a test plan and a testbed for performance analysis of MEMS-based IMUs under vibration conditions,” *Measurement*, vol. 158, p. 107734, Jul. 2020, DOI: 10.1016/j.measurement.2020.107734
- [18] IEC 60068-2-6, “Environmental testing - Part 2-6: Tests - Test Fc: Vibration (sinusoidal).” International Electrotechnical Commission, 2009.
- [19] JEDEC Solid State Technology, “JEDEC STANDARD: Vibration, Variable Frequency.” JESD22-B103B.01, 2016.
- [20] MIL-STD-810G, “Environmental Engineering Considerations and Laboratory Tests,” no. October. US Department of Defense, Washington DC, 2008.
- [21] STMicroelectronics, “STM32 Nucleo-64 boards user manual.” Revision 13, 2019.
- [22] S. O. H. Madgwick, A. J. L. Harrison, and R. Vaidyanathan, “Estimation of IMU and MARG orientation using a gradient descent algorithm,” in *2011 IEEE International Conference on Rehabilitation Robotics*, 2011, pp. 1–7.